Numerical models in aquacultural engineering:two examples

Raman-Nair, W.; Colbourne, D. B.; Gagnon, M.; Bergeron, P.

Publisher's version / Version de l'éditeur:

8th Canadian Marine Hydromechanics and Structures Conference [Proceedings], 2007

NUMERICAL MODELS IN AQUACULTURAL ENGINEERING : TWO EXAMPLES

W. Raman-Nair *, **B. Colbourne** *, **M.Gagnon** **, **P. Bergeron** **.

* *Institute for Ocean Technology, National Research Council, Arctic Ave.,St.John's, NL, Canada, A1B 3T5*
** *Biorex Inc., 295,ch. Sainte Foy,Quebec,QC, Canada,G1R1T5*

Abstract: Dynamic models are described for two applications in aquacultural engineering : mussel longline systems and fish nets. The mussel longline is modeled using lumped masses and tension-only springs. The mussel culture and attached buoys are modeled as cylinders attached to the main line. The fish net is modeled as an inter-connected system of lumped masses and tension-only springs. Surface waves are described by Stokes' second order wave theory. The hydrodynamic loads are applied via a Morison's equation approach using the instantaneous relative velocities and accelerations between the fluid field and the structural system. The equations of motion are formulated for the coupled dynamics of the masses in each system.

Keywords: Mussel longline, fish net, numerical model, aquacultural engineering

1. INTRODUCTION

The shortages in wild fish stocks due to overfishing has created an urgent need for aquaculture which has become a versatile industry encompassing a wide range of methods. Although fish farming is usually carried out in coastal areas, the aquaculture industry is considering the move to more exposed areas with cleaner and deeper waters which is beneficial for the health of the product. The more severe environmental conditions in such open areas requires the evaluation of the forces and motions experienced by the aquaculture installations in order to provide safe designs and reduce the likelihood of structural failure. In this paper we provide brief descriptions of numerical modeling of two typical structures :(a) a mussel longline and (b) a fish net

2. MUSSEL LONGLINE SYSTEM

With the collaboration of the environmental consulting firm Biorex Inc. (Quebec, Canada), the authors have undertaken a significant extension of their previous work on the numerical modeling of aquaculture longline configurations which are based on arrangements found in operating shellfish farms located in the Gulf of St. Lawrence in Canada. In our previous work, the main line was modeled using a lumped parameter representation of cable dynamics with the effects of all attachments (buoys, mussel culture, concrete weights) modeled as applied loads. The present study involves the *coupled dynamics* of the main line and the attached buoys and mussel culture. The dynamics of the concrete blocks is not modeled and their effect on the main line is applied via a line stiffness. The simulations can be used to determine the configuration of a longline system in current and waves and to assess the loads ap-

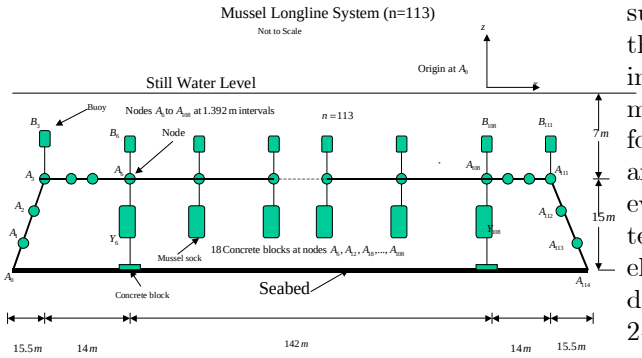

Fig. 1. System Configuration

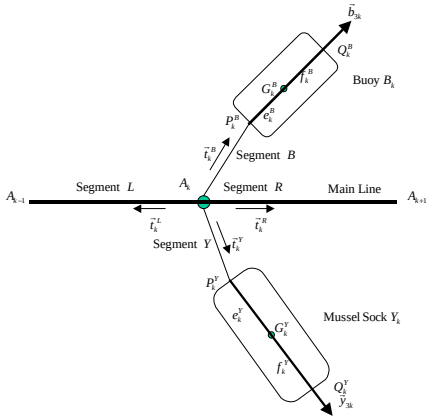

Fig. 2. Sub-system S_k

pearing at the anchoring points, thus evaluating the adequacy of the anchors and identifying the potential for anchor slippage (or dragging). It is expedient to use Kane's equations (Kane and Levinson,1985) for formulating the equations of motion for this multibody system. We present the results of some simulations predicting the loads in and shapes assumed by the longlines under various loading scenarios. We assume that the hydrodynamic loads are due primarily to added-mass effects and drag. In this regard, we allow for loading due to an arbitrary fluid velocity and acceleration field which is assumed to be undisturbed by the system. This allows for the inclusion of wave and current effects via the use of the Morison et al. approach (Chakrabarti,1987). A series of experimental trials was conducted by Biorex Inc. and the Institute for Ocean Technology to directly measure the drag of key components of the shellfish longline structures.

A diagram of a typical mussel longline system is given in Fig. 1 The origin of inertial coordinates is an arbitrary point O and the inertial frame is denoted by N with unit vectors $\overrightarrow{N}_1, \overrightarrow{N}_2, \overrightarrow{N}_3$. The longline is anchored at points A_0 and A_{n+1} and is composed of an assembly of the sub-systems S_k $(k = 1, \ldots, n)$ illustrated in Fig. 2 Subsystem S_k consists of node A_k on the main line with an attached buoy B_k (sphere or cylinder) and suspended cylinder Y_k. In addition, the mass of the segment halves on either side of node A_k is included in the lumped mass at the node. The main line segments as well as the attachment lines for buoys, mussel cultures and concrete weights are modeled as springs. A spring stiffness k is evaluated as $k = \frac{AE}{\ell}$, where A is the line material cross-sectional area, E is its modulus of elasticity and ℓ is the unstretched length. A spring damping coefficient c is estimated as $c = \zeta \times 2\sqrt{k \times \text{ segment mass}}$, where ζ is the damping ratio which lies between 0 and 1. Since there are no attachments on the anchor lines, the stiffness and damping of the attachment lines for buoys and mussel cultures are set to zero in sub-systems S_1, S_2, S_{n-1} and S_n. Corner buoys B_3 and B_{n-2} are attached to nodes A_3 and A_{n-2} respectively and since there are no mussel cultures at these nodes, the stiffness and damping of the mussel culture attachment lines are set at zero in sub-systems S_3 and S_{n-2}. An arbitrary orientation of a rigid body B can be specified by employing space-three 1-2-3 orientation angles θ_i $(i = 1, 2, 3)$ defined as follows (Kane,Likins and Levinson,1983). Beginning with body-fixed axes $\overrightarrow{b}_i$ aligned with $\overrightarrow{N}_i$ $(i = 1, 2, 3)$ we rotate B successively about $\overrightarrow{N}_1, \overrightarrow{N}_2, \overrightarrow{N}_3$ by angles $\theta_1, \theta_2, \theta_3$ respectively. The body-fixed unit vectors $\overrightarrow{b}_i$ are then related to the inertial unit vectors $\overrightarrow{N}_i$ by

$$\begin{pmatrix} \overrightarrow{N}_1 \\ \overrightarrow{N}_2 \\ \overrightarrow{N}_3 \end{pmatrix} = \left[{}^N C^B\right] \begin{pmatrix} \overrightarrow{b}_1 \\ \overrightarrow{b}_2 \\ \overrightarrow{b}_3 \end{pmatrix} \tag{1}$$

where the orthogonal transformation matrix $\left[{}^N C^B\right]$ is called the space-three 1-2-3 rotation matrix and is given by (Kane,Likins and Levinson, 1983)

$$\left[{}^N C^B\right] = \begin{pmatrix} c_2c_3 & s_1s_2c_3 - s_3c_1 & c_1s_2c_3 + s_3s_1 \\ c_2s_3 & s_1s_2s_3 + c_3c_1 & c_1s_2s_3 - c_3s_1 \\ -s_2 & s_1c_2 & c_1c_2 \end{pmatrix} \tag{2}$$

with $s_i = \sin\theta_i$, $c_i = \cos\theta_i$ $(i = 1, 2, 3)$. In this way, the orientation of the rigid bodies B_k and Y_k is specified by using body-fixed axes with unit vectors $\overrightarrow{b}_{ik}$ and $\overrightarrow{y}_{ik}$ respectively $(i = 1, 2, 3)$ at the centres of mass. Sub-system S_k has 15 generalised coordinates defined as follows :

- Node A_k : inertial coordinates q^A_{ik} $(i = 1, 2, 3)$
- Buoy B_k : orientation angles $q^B_{ik} = \theta^B_{ik}$ $(i = 1, 2, 3)$ and body-frame coordinates of centre of mass $q^B_{i+3,k}$ $(i = 1, 2, 3)$
- Mussel Culture Y_k : orientation angles $q^Y_{ik} = \theta^Y_{ik}$ $(i = 1, 2, 3)$ and body-frame coordinates of centre of mass $q^Y_{i+3,k}$ $(i = 1, 2, 3)$

The orientation angles are the space-three 1-2-3 angles of rigid body orientation (Kane,Likins

and Levinson, 1983). There are 15 corresponding generalised speeds defined as

- Node A_k : inertial velocity components $u_{ik}^A = \overrightarrow{v}^{A_k} \cdot \overrightarrow{N}_i \ \ (i = 1, 2, 3)$, where $\overrightarrow{v}^{A_k}$ is the velocity of A_k
- Buoy B_k : body-frame angular velocity components $u_{ik}^B = \overrightarrow{\omega}^{B_k} \cdot \overrightarrow{b}_{ik} \ \ (i = 1, 2, 3)$, and body-frame velocity components of the centre of mass $u_{i+3,k}^B = \overrightarrow{v}^{B_k} \cdot \overrightarrow{b}_{ik} \ \ (i = 1, 2, 3)$, where $\overrightarrow{\omega}^{B_k}$ is the angular velocity and $\overrightarrow{v}^{B_k}$ is the velocity of the centre of mass of B_k
- Mussel Culture Y_k : body-frame angular velocity components $u_{ik}^Y = \overrightarrow{\omega}^{Y_k} \cdot \overrightarrow{y}_{ik} \ \ (i = 1, 2, 3)$, and body-frame velocity components of the centre of mass $u_{i+3,k}^Y = \overrightarrow{v}^{Y_k} \cdot \overrightarrow{y}_{ik} \ \ (i = 1, 2, 3)$, where $\overrightarrow{\omega}^{Y_k}$ is the angular velocity and $\overrightarrow{v}^{Y_k}$ is the velocity of the centre of mass of Y_k.

The generalised coordinates $q_{ik}^S$and generalised speeds $u_{ik}^S$of sub-system S_k are then labelled as follows :

$$\begin{array}{rl} q_{ik}^S = q_{ik}^A \ ; \ u_{ik}^S = u_{ik}^A & (i = 1, 2, 3) \\ q_{3+i,k}^S = q_{ik}^B \ ; \ u_{3+i,k}^S = u_{ik}^B & (i = 1, \ldots, 6) \\ q_{9+i,k}^S = q_{ik}^Y \ ; \ u_{9+i,k}^S = u_{ik}^Y & (i = 1, \ldots, 6) \end{array} \quad (3)$$

2.1 Forces on node A_k

The system is subjected to gravity and fluid forces. The fluid field is described by either a current velocity field or a wave velocity and acceleration field (in directions N_1 and N_2) using standard formulae for a Stokes second order wave. The generalised inertia force on node A_k is

$$F_r^{*A_k} = \overrightarrow{v}_r^{A_k} \cdot \left(-m_k^A \overrightarrow{a}^{A_k}\right) \quad (4)$$

where $\overrightarrow{a}^{A_k}$ is the acceleration, $\overrightarrow{v}_r^{A_k}$ is the partial velocity and m_k^A is the mass of node A_k. The net non-inertial force $\overrightarrow{F}^{\mathrm{net}/A_k}$on node A_k is the sum of the forces due to gravity, buoyancy, fluid drag, line tensions and structural damping as described below. The generalised active force is then

$$F_r^{A_k} = \overrightarrow{F}^{\mathrm{net}/A_k} \cdot \overrightarrow{v}_r^{A_k} \quad (r = 1, \ldots, 15) \quad (5)$$

If the volume of node A_k is V_k^A, the net force on node A_k due to gravity and buoyancy is

$$\overrightarrow{F}^{GB/A_k} = \left(\rho_f V_k^A - m_k^A\right) g \ \overrightarrow{N}_3 \quad (6)$$

where g is the acceleration due to gravity.

There are four line segments attached to node A_k as shown in Fig. 2. The segments are identified by superscripts L, R, B and Y and we allow for line tension but not compression. For example, if the unstretched length of segment $A_{k-1}A_k$ is ℓ_k^L, the unit vector along $\overrightarrow{A_k A_{k-1}}$ is $\overrightarrow{t}_k^L$, and the instantaneous length is Z_{4k}^L, the tensile force on node A_k is calculated as $k_k^L Z_{5k}^L \overrightarrow{t}_k^L$ where k_k^L is the line stiffness and Z_{5k}^L is the line extension computed as

$$Z_{5k}^L = \frac{1}{2}\left\{\left(Z_{4k} - \ell_k^L\right) + \left|Z_{4k} - \ell_k^L\right|\right\} \quad (k = 1, \ldots, n) \quad (7)$$

Similarly, the structural damping force in segment $A_{k-1}A_k$ on node A_k is $c_k^L Z_{6k}^L \overrightarrow{t}_k^L$ where c_k^L is the line damping coefficient and Z_{6k}^L is the velocity of A_{k-1}relative to A_k computed as

$$Z_{6k}^L = \sum_{i=1}^{3} \left(u_{i,k-1}^A - u_{ik}^A\right) t_{ik}^A \ \mathrm{sign}\left(Z_{5k}^L\right) \quad (k = 1, \ldots, n) \quad (8)$$

where t_{ik}^A is the i th component of $\overrightarrow{t}_k^L$. Using similar notation for the other segments, we write the tensile force $\overrightarrow{F}^{T/A_k}$ and structural damping force $\overrightarrow{F}^{SD/A_k}$on node A_k as

$$\overrightarrow{F}^{T/A_k} = k_k^L Z_{5k}^L \overrightarrow{t}_k^L + k_k^R Z_{5k}^R \overrightarrow{t}_k^R + k_k^B Z_{5k}^B \overrightarrow{t}_k^B + k_k^Y Z_{5k}^Y \overrightarrow{t}_k^Y \quad (9)$$

$$\overrightarrow{F}^{SD/A_k} = c_k^L Z_{6k}^L \overrightarrow{t}_k^L + c_k^R Z_{6k}^R \overrightarrow{t}_k^R + c_k^B Z_{6k}^B \overrightarrow{t}_k^B + c_k^Y Z_{6k}^Y \overrightarrow{t}_k^Y \quad (10)$$

We note that the above computations for segments B and Y involve the coordinates and velocities of the corresponding buoy and mussel sock.

The force on node A_k due to fluid drag is denoted by $\overrightarrow{F}^{D/A_k}$ and is due primarily to the drag force on half of segments A_kA_{k-1} and A_kA_{k+1}, denoted by $\overrightarrow{F}^{DL/A_k}$ and $\overrightarrow{F}^{DR/A_k}$ respectively. If $\overrightarrow{v}_k^f$ is the fluid velocity at node A_k, the velocity of the fluid relative to A_k is $\overrightarrow{v}_k^{\mathrm{Rel}} = \overrightarrow{v}_k^f - \overrightarrow{v}^{A_k}$ which has components tangential and normal to segment A_kA_{k-1} given respectively by

$$\overrightarrow{v}_k^{\mathrm{Rel}/t^L} = \overrightarrow{v}_k^{\mathrm{Rel}} \cdot \overrightarrow{t}_k^L \ ; \ \ \overrightarrow{v}_k^{\mathrm{Rel}/n^L} = \overrightarrow{v}_k^{\mathrm{Rel}} - \overrightarrow{v}_k^{\mathrm{Rel}/t^L} \quad (11)$$

We compute the drag force on half of segment A_kA_{k-1} as

$$\overrightarrow{F}^{DL/A_k} = \frac{1}{4}\rho_f A_T C_{DT} \left|\overrightarrow{v}_k^{\mathrm{Rel}/t^L}\right| \overrightarrow{v}_k^{\mathrm{Rel}/t^L} + \frac{1}{4}\rho_f A_N C_{DN} \left|\overrightarrow{v}_k^{\mathrm{Rel}/n^L}\right| \overrightarrow{v}_k^{\mathrm{Rel}/n^L} \quad (12)$$

where C_{DT} and C_{DN} are tangential and normal drag coefficients, and $A_T = \pi d \ Z_{4k}^L$, $A_N = d \ Z_{4k}^L$ are the associated areas. The drag force $\overrightarrow{F}^{DR/A_k}$ is computed in a similar fashion and the drag on node A_k is then

$$\overrightarrow{F}^{D/A_k} = \overrightarrow{F}^{DL/A_k} + \overrightarrow{F}^{DR/A_k} \quad (13)$$

If node A_k on the main line is connected to a concrete block on the seabed, the unit vector from

the instantaneous position of the node to the original postion of the block is denoted by $\overrightarrow{t}_k^{\text{conc}}$. The line tension directed along this vector is denoted by $\overrightarrow{T}_k^{\text{conc}}$ and calculated in the same way as the tension in other lines. Its vertical component (direction $\overrightarrow{N}_3$) is denoted by $T_k^{V,\text{conc}}$ and its horizontal component (resultant of components in directions $\overrightarrow{N}_1$ and $\overrightarrow{N}_2$) is denoted by $T_k^{H,\text{conc}}$. From elementary statics, the concrete block will slip when

$$T_k^{H,\text{conc}} + \mu_s T_k^{V,\text{conc}} = \mu_s W_{\text{conc}} \qquad (14)$$

where μ_s is the seabed friction coefficient and W_{conc} is the submerged weight of the concrete block. After slip, we assume that the block slides freely and the tension in the concrete attachment line is directed vertically downwards from node A_k. Structural damping in the concrete attachment lines is calculated in the same way as in other lines. The net force (tension and damping) on A_k due to the concrete block is denoted by $\overrightarrow{F}^{C/A_k}$.

2.2 Forces on Mussel Socks and Buoys

We will describe the computation for a mussel sock. The procedure for the buoys is similar. The generalised inertia force (non-hydrodynamic) on mussel sock Y_k is $F_r^{*NH/Y_k} = \overrightarrow{\omega}_r^{Y_k} \cdot \overrightarrow{T}^{*Y_K} + \overrightarrow{v}_r^{G_k^Y} \cdot (-m_k^Y \overrightarrow{a}^{G_k^Y})$ where $\overrightarrow{T}^{*Y_K}$ is the inertia couple on Y_k, $\overrightarrow{\omega}_r^{Y_k}$ is the partial angular velocity, $\overrightarrow{v}_r^{G_k^Y}$ is the partial velocity of the mass centre, $\overrightarrow{a}^{G_k^Y}$ is the acceleration of the mass centreand, m_k^Y is its mass. This can be evaluated in the form

$$F_r^{*NH/Y_k} = -V_{rk}^Y \overset{S}{\dot{u}}_{rk} + \phi_{rk}^Y \quad (r = 1, \ldots, 15) \qquad (15)$$

The inertial force on Y_k due to added mass is denoted by $\overrightarrow{H}^{A/Y_k}$ and written in the Y_k frame as (Brennen,1982; Landau and Lifshitz,1959)

$$\{H^A\} = -[A]\{a^Y\} \qquad (16)$$

where $[A]$ is the added-mass matrix in the Y_k frame and $\{a^Y\}$ is the body acceleration vector in the Y_k frame. The generalised inertia force due to added-mass is $F_r^{*A/Y_k} = \overrightarrow{H}^{A/Y_k} \cdot \overrightarrow{v}_r^{G_k^Y}$ and can be evaluated in the form

$$F_r^{*A/Y_k} = -W_{rk}^Y \overset{S}{\dot{u}}_{rk} + \psi_{rk}^Y \qquad (17)$$
$$(r = 1, \ldots, 15; \quad k = 1, \ldots, n)$$

The generalised inertia force on Y_k is the sum of the non-hydrodynamic and added-mass components, i.e.

$$F_r^{*Y_k} = F_r^{*NH/Y_k} + F_r^{*A/Y_k} \qquad (18)$$
$$(r = 1, \ldots, 15; \quad k = 1, \ldots, n)$$

The generalised active force on Y_k due to gravity and buoyancy is $F_r^{GB/Y_k} = \overrightarrow{v}_r^{G_k^Y} \cdot (\rho_f V_k^Y - m_k^Y) g \overrightarrow{N}_3$.

To account for seabed touchdown, we note that the bottom point Q_k^Y of mussel sock Y_k is specified by the distance f_k^Y from this point to the centre of mass, and the body axis $\overrightarrow{y}_{3k}$. The height of the mussel sock above the seabed is then

$$h_k^Y = C_{31,k}^Y q_{4k}^Y + C_{32,k}^Y q_{5k}^Y + C_{33,k}^Y (q_{6k}^Y + f_k^Y) \qquad (19)$$

where $C_{ij,k}^Y$ is the $i-j$ element of the matrix 2 associated with body Y_k. At seabed touchdown, the normal reaction force is $R_k^Y \overrightarrow{N}_3$ where

$$R_k^Y = \frac{1}{2} k_E \left(\left| h_k^Y \right| - h_k^Y \right) \qquad (20)$$

and k_E is the seabed stiffness (resistance to penetration). We note that R_k^Y is zero when $h_k^Y > 0$. The generalised active force due to touchdown is $F_r^{TD/Y_k} = R_k^Y \overrightarrow{N}_3 \cdot \overrightarrow{v}_r^{Q_k^Y}$

The tension in the mussel sock attachment line depends on the extension in the line and the damping depends on the relative velocity between the attachment point P_k^Y and node A_k on the main line. Using notation similar to that used for the main line, the generalised active force on Y_k due to tension and structural damping is then

$$F_r^{TSD/Y_k} = \left(-k_k^Y Z_{5k}^Y - c_k^Y Z_{6k}^Y \right) \overrightarrow{t}_k^Y \cdot \overrightarrow{v}_r^{P_k^Y} \qquad (21)$$

The velocity of the fluid relative to sock Y_k is

$$\overrightarrow{U}_k^{\text{Rel}} = \sum U_{ik}^{\text{Rel}} \overrightarrow{y}_{ik} \qquad (22)$$

where U_{ik}^{Rel} is the difference between the fluid velocity and the velocity of the centre of mass of Y_k, both expressed in the Y_k frame. The tangential drag force acts in the direction $\overrightarrow{y}_{3k}$. The normal drag force acts in the direction of the unit vector normal to $\overrightarrow{y}_{3k}$ in the plane defined by $\overrightarrow{U}_k^{\text{Rel}}$ and $\overrightarrow{y}_{3k}$. The tangential and normal drag coefficients are denoted by C_{DT} and C_{DN} with associated areas A_T ($\pi\times$ diameter $\times$ length) and A_N (length $\times$ diameter). The drag force on mussel sock Y_k can then be written in the form

$$\overrightarrow{F}^{D/Y_k} = \sum_{i=1}^{3} \alpha_{ik}^Y \overrightarrow{y}_{ik} \qquad (23)$$

The generalised active force is $F_r^{D/Y_k} = \overrightarrow{F}^{D/Y_k} \cdot \overrightarrow{v}_r^{G_k^Y}$

The forces $\overrightarrow{H}^{Y_k}$ on mussel sock Y_k due to the fluid inertia is denoted by $\overrightarrow{H}^{I/Y_k}$ and is written in the form (Brennen,1982; Landau and Lifshitz,1959)

$$\{H^I\} = \left(\rho_f V_k^Y [I] + [A] \right) \{a^F\} \qquad (24)$$

where $[A]$ is the added-mass matrix in the Y_k frame, V_k^Y is the volume of Y_k, $[I]$ is the 3×3 identity matrix, and$\{a^F\}$ is the fluid acceleration vector in the Y_k frame. The generalised active force due to fluid inertia is $F_r^{I/Y_k} = \overrightarrow{H}^{I/Y_k} \cdot \overrightarrow{v}_r^{G_k^Y}$

2.3 Equations of Motion

The generalised inertia and active forces for sub-system S_k (Fig. 2) are assembled as

$$\begin{aligned} F_{rk}^{*S} &= F_r^{*A_k} + F_r^{*B_k} + F_r^{*Y_k} \\ F_{rk}^{S} &= F_r^{A_k} + F_r^{B_k} + F_r^{Y_k} \\ (r = 1, \ldots, 15; \quad & k = 1, \ldots, n) \end{aligned} \tag{25}$$

where superscripts A, B and Y refer to the main line, buoy and mussel sock respectively and superscript S refers to sub-system S_k. In order to solve for the accelerations, the generalised inertia forces are written in the form

$$\begin{aligned} F_{rk}^{*S} &= -M_{rk}^{S} \dot{u}_{rk}^{S} + b_{rk}^{S} \\ (r = 1, \ldots, 15; \quad & k = 1, \ldots, n) \end{aligned} \tag{26}$$

The equations of motion are assembled for the entire system (superscript sys)and are written as (Kane and Levinson,1985)

$$F_r^{*sys} + F_r^{sys} = 0 \qquad (r = 1, \ldots, 15n) \tag{27}$$

which is re-arranged in the form

$$\dot{u}_r^{sys} = \frac{1}{M_r^{sys}} \left(F_r^{sys} + b_r^{sys}\right) \qquad (r = 1, \ldots, 15n) \tag{28}$$

We define the $30n \times 1$ vector $\{x\}$ as

$$\{x\} = \begin{pmatrix} \{q\}^{sys} \\ \{u\}^{sys} \end{pmatrix} \tag{29}$$

and the coupled set of ordinary differential equations to be solved is written as $\left\{\dot{x}\right\} = \{f(t, \{x\}\}$. The components of the vector function f are given by the quantities $\dot{q}_r^{sys}$ and equation (28). The equations are solved by the MATLAB Runge-Kutta routine ode45 with appropriate initial conditions.

3. TEST PROBLEM

We consider the simple system, illustrated in Fig. 3, consisting of two nodes on the mainline each carrying a buoy and mussel sock. Each of segments OA, AB, BC has stiffness k and unstretched length L_0. The submerged weight of each mussel sock is W_Y and of each mainline node is W_A. The buoyancy of each buoy is F_B acting upwards.

3.1 Static Equilibrium (no waves or current)

The net upward force on each node is therefore $F = F_B - (W_A + W_Y)$. At static equilibrium we

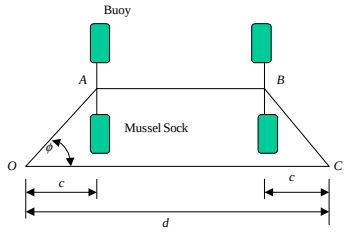

Fig. 3. Test Problem ($n = 2$)

can show that the angle ϕ between OA or BC and the horizontal satisfies the relation

$$\frac{3F}{2kL_0} = \left(\frac{d - L_0}{2L_0}\right) \tan\phi - \sin\phi \tag{30}$$

and the tension T in segments OA, BC is $T = \frac{F}{\sin\phi}$.

3.2 Mussel Sock Orientation in Current

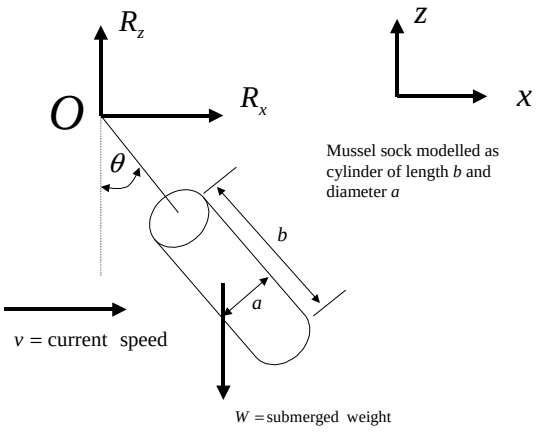

Fig. 4. Cylinder Suspended in Steady Current

The mussel sock is modelled as a cylinder of length b, diameter a, submerged weight W, suspended from point O in a uniform current of speed v as shown in Fig. 4. At equilibrium, the sock is inclined at an angle θ to the vertical as shown. The normal drag coefficient (i.e. for flow normal to the length) is denoted by C_{DN}. The associated area is $A_N = ab$. The tangential drag coefficient (i.e. for flow parallel to the length) is denoted by C_{DT}. The associated area is $A_T = \pi ab$. We assume that the cylinder ends are tapered and hence the

end areas ($\pi a^2/4$) do not offer flow resistance. The fluid density is ρ_f. Define the dimensionless parameter α by

$$\alpha = \frac{2W}{\rho_f a b C_{DN} v^2} \tag{31}$$

Then the angle θ is given by

$$\theta = \sin^{-1}\left\{\frac{-\alpha + \sqrt{\alpha^2+4}}{2}\right\} \tag{32}$$

The horizontal and vertical components ($R_x,\ R_z$) of the supporting force at O are given by

$$\frac{R_x}{W} = -\frac{1}{\alpha}\left(\beta \sin^3\theta + \cos^3\theta\right) \tag{33}$$

$$\frac{R_z}{W} = 1 + \frac{1}{\alpha}\left(\beta \sin^2\theta\cos\theta - \cos^2\theta\sin\theta\right) \tag{34}$$

where

$$\beta = \frac{\pi C_{DT}}{C_{DN}} \tag{35}$$

We first determine α from (31) and then find θ from (32). Then R_x and R_z are found from (33) and (34).

3.3 Simulation Results (Test problem)

A simulation was conducted for the following parameters (which are not intended to represent a real system). The mainline has unstretched length 10 m, diameter 20 mm, mass per unit length 0.25 kg/m, modulus of elasticity $1MPa$. The distance between the anchors is $d = 11$ m. Each buoy B_k and mussel sock Y_k is a solid cylinder of length 1 m, diameter 0.2 m. The density of B_k is 100 kg/m^3 and the density of Y_k is 1500 kg/m^3. The normal and tangential drag coefficients are $C_{DN} = 1.2$, $C_{DT} = 0.1$. The stiffness of each mainline segment is found as $k = 94.2478$ N/m and the net upward force on each node in static equilibrium is found as $F = 141.0404$ N. From the simulation results at steady state with no waves or current we find that the distance c (Fig.3) is 3.2435 m and the mainline is at a height of 4.1141 m above the seabed. This gives $\phi = 0.9032$ rad. The tension T iscomputed from the line stiffness and line extension as $T = 179.5942$ m. To check, we solve equation (30) numerically to find that $\phi = 0.9032$ rad and we find $T = \frac{F}{\sin\phi} = 179.5979$ N. For the case of a 1 m/s steady current in the x direction the simulation results at steady state give the longitudinal unit vector $\overrightarrow{y}_3$ of each mussel sock as (0.5686, 0, −0.8226). To check, we use (32) to find $\theta = 34.6516^0$ from which we compute the longitudinal unit vector as $(\sin\theta,\ 0,\ -\cos\theta) = (0.5686,\ 0,\ -0.8226)$.

3.4 Typical Results

The design of a typical longline used by mussel farmers in Cascapedia Bay, Quebec is described below based on information they provided to Biorex Inc. and the data collected by Biorex on their culture gears. A diagram of the system is illustrated in Fig. 1. The longline has distance 201 m between the anchors. The line has diameter 0.019 m, weight per unit length (in air) without biofouling 0.19 kg/m, modulus of elasticity $1\ GPa$. The longline is modeled by $n = 113$ nodes, labelled A_k, $(k = 1, \ldots, n)$. There are 2 nodes on each anchor line and 109 nodes on the main line. Buoys, labelled B_k, and mussel socks, labelled Y_k, are attached to the main line nodes A_6 to A_{108}. Concrete blocks (weight in air of 145 kg each, density 2380 kg/m^3) are attached to the main line at points $A_6, A_{12}, A_{18}, \ldots, A_{108}$. The location of the concrete blocks is specified as vertically below the initial mainline node positions. The mussel socks are modeled as cylinders and the weight in air of each mussel sock is 140 kg. The mussel weight conversion factor $f = 5.4$ is used to calculate the specific gravity and mussel sock volume. Each cylinder Y_k has length 4 m and diameter 0.424 m, representing two loops of sock. The buoys on the central part of the main line (buoys B_6 to B_{108}) are all spherical. Most of these buoys have weight in air 3.9 kg, diameter 0.4 m , drag coefficient 0.7 and specified buoyancy 34.5 kg. The exceptions are as follows. Buoys at nodes $9, 15, 21, \ldots, 105$ have weight in air 1.7 kg, diameter 0.3 m, drag coefficient 0.7 and buoyancy 14.8 kg. Two spherical buoys (combined weight in air 7.8 kg and buoyancy 69 kg) are attached at each node where a concrete block is located. The corner buoys at nodes 3 and 111 are actually 3 buoys (each) but for the simulation are modeled as single buoys B_3 and B_{111}. Owing to biofouling, the corner buoys B_3 and B_{111} have weight in air of 83.1 kg, diameter 1.2 m ,drag coefficient 3.9 and buoyancy 87.7 kg. The weight in water of line segments is calculated using the weight conversion factor for biofouled segments and weight of displaced water for clean segments. A segment is identified as clean if the value entered for the biofouled weight per unit length is equal to the clean weight per unit length. The biofouled portions are from the anchors to node 6 on the left node 108 on the right, these sections having diameter 0.154 m and weight in air 12 kg/m. To account for biofouling of the concrete attachment lines, the weight in air of the mussel socks at each concrete block location is increased by 35 kg. A seabed friction coefficient $\mu_s = 0.3$ is assumed to specify a slip criterion for the blocks in current.

The profile of the system with a 0.21 m/s current in the y direction is shown in Fig. 5 (450 sec.

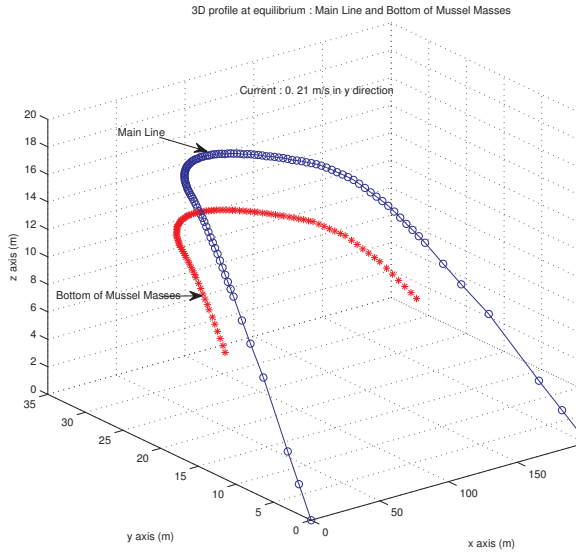

Fig. 5. Equilibrium profile under y-direction current

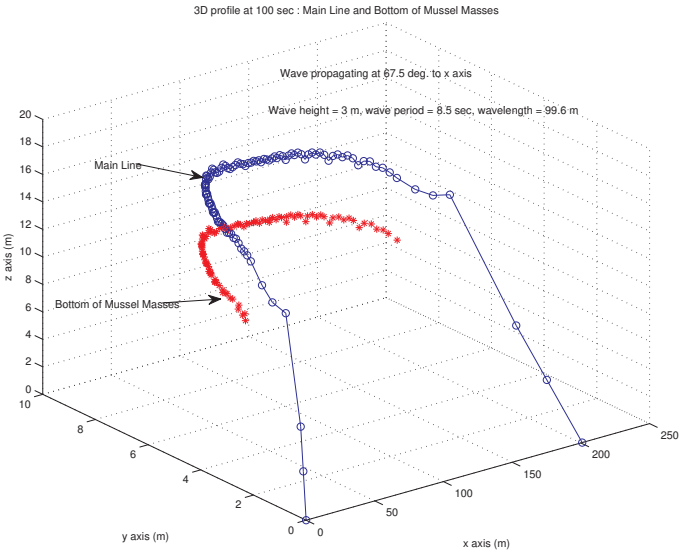

Fig. 6. Instantaneous profile at 100 sec under wave loading

simulation). The tensions at the anchors are (x, y and z components)

$$T_{\text{left anchor}} = \begin{pmatrix} 6.4 \\ 3.4 \\ 2.5 \end{pmatrix} \times 10^3 \ N \qquad (36)$$

$$T_{\text{right anchor}} = \begin{pmatrix} -6.4 \\ 3.4 \\ 2.5 \end{pmatrix} \times 10^3 \ N \qquad (37)$$

The central part of the main line is deviated 32 m in the y direction. The lower end of the lowest socks (Y_6 and Y_{108}) is 6.8 m above the seabed. Mussel sock Y_{10} makes an angle of 13.2^0 with the *downward* vertical. This result can be verified by using the formula (32).

A simulation was also performed with a wave of height 3 m , period 8.5 sec, and wavelength 99.6 m propagating at angle 67.5^0 with the positive x direction. The instantaneous profile at 100 sec is shown in Fig.6 The tensions at the anchors are shown in Fig.7

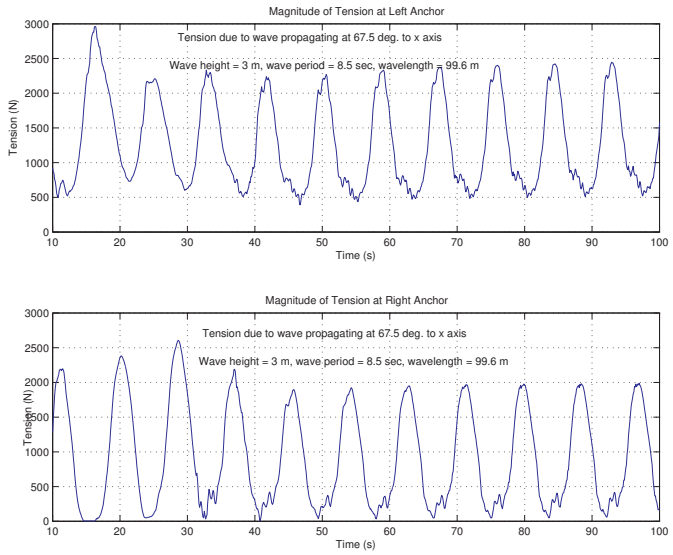

Fig. 7. Wave induced tensions at anchors

4. MODEL OF FISH NET

The net is modeled by longitudinal lines L^α $(\alpha = 1, \ldots, \nu)$ and transverse lines J^k $(k = 1, \ldots, n)$ with a spherical knot at the intersection points (nodes) $A^{k\alpha}$ at each intersection, as shown in Fig.(8). The mass of the line segments is lumped in halves at the nodes and the elasticity of the lines is modeled by linear springs. The net is attached to supporting points (which may be moving) $A^{0,\alpha}$, $A^{n+1,\alpha}$ $(\alpha = 1, \ldots, \nu)$ and $A^{k,0}$, $A^{k,\nu+1}$ $(k = 1, \ldots, n)$ .The Cartesian coordinates of the supporting points may be specified functions of time t. We denote the Cartesian coordinates of the lumped mass $A^{k\alpha}$ by $c_i^{k\alpha}$ $(k = 1, \ldots n;\ \alpha = 1, \ldots \nu;\ i = 1, 2, 3)$ and define the generalised coordinates as q_r $(r = 1, \ldots, 3n\nu)$ where

$$c_i^{k\alpha}(t) = q_{3n(\alpha-1)+3(k-1)+i}$$
$$(k = 1, \ldots n;\ \alpha = 1, \ldots \nu;\ i = 1, 2, 3) \qquad (38)$$

The generalised speeds are defined as $u_r = \dot{q}_r$ $(r = 1, \ldots 3n\nu)$. The forces on the line segments (structural and hydrodynamic) are applied in the same way as described for the mussel longline model above and the equatins of motion assembled by equating the sum of generalised inertia and active forces to zero. We define the $6n\nu$ dimensional vector $\{x\}$ as in equation 29) and the equations of motion written as before in the form $\left\{\dot{x}\right\} = \{f(t, \{x\}\}$. The solution is obtained

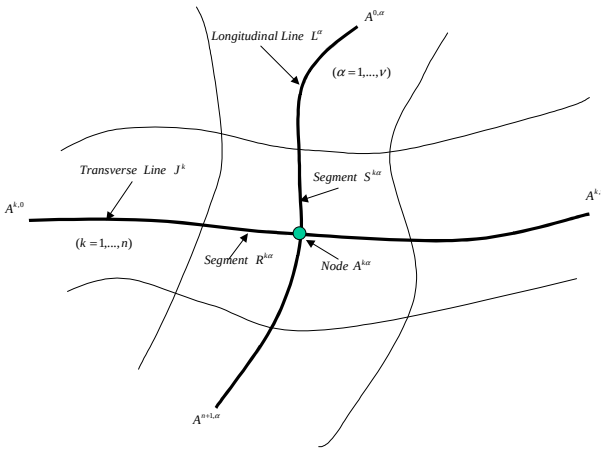

Fig. 8. Net Model

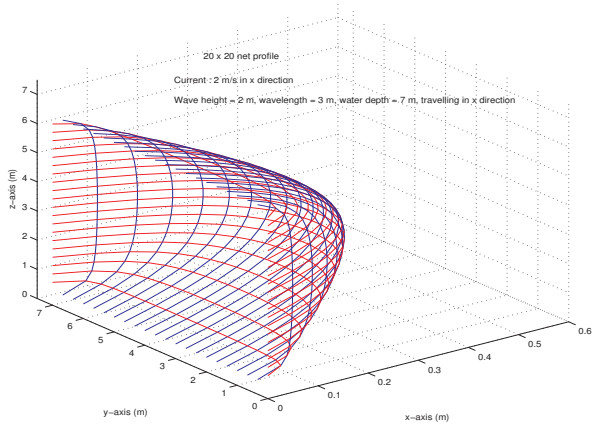

Fig. 9. Net profile

numerically. Fig.(9) is example of the instantaneous profile of a 20×20 net (i.e. 20 longitudinal and 20 transverse lines) in a 2 m/s x direction current and a wave of height 2 m, wavelength 3 m propagating in the x direction. The tension in each segment of the net is computed from the line stiffness and the nodal displacements.

5. CONCLUSIONS

Numerical models of the three dimensional dynamics of a submerged mussel longline system and a fish net have been presented. The method is based on Kane's formalism which is well known to provide an efficient way of formulating the equations of motion of multibody systems. The numerical model of the mussel longline is currently being used by Biorex Inc. to predict the dynamics of longline systems in Quebec, Canada. We expect that the results will be useful for checking and optimizing shellfish aquaculture designs prior to installation and for modifying existing designs to safeguard against failure. The net model is currently being evaluated by experimental tests at the Institute for Ocean Technology.

Acknowledgements

This mussel longline project was partly funded by the Société de l'Industrie maricole du Québec inc. (SODIM) and two provincial departments (Quebec Canada), Agriculture, Pêcheries et Alimentation (MAPAQ) and Développement économique, Innovation et Exportation (MDEIE).

References

Brennen,C.E.,1982, A Review of Added Mass and Fluid Inertial Forces, Report CR 82.010, Naval Civil Engineering Laboratory, Port Hueneme, California

Chakrabarti,S.K.,1987, Hydrodynamics of Offshore Structures (Springer Verlag).

Kane,T.R., Levinson,D.A.,1985, Dynamics : Theory and Applications (McGraw Hill Inc.).

Kane,T.R., Likins,P.W., Levinson,D.A.,1983, Spacecraft Dynamics (McGraw Hill Inc.), pp 30.

Landau,L.D., Lifshitz,E.M.,1959, Fluid Mechanics (Pergamon Press), pp 35.

MATLAB version 2007a, MathWorks Inc.,Natick,MA,USA.

Raman-Nair,W. and Colbourne,B., 2003, Vol. 27,Dynamics of a Mussel Longline System, Aquacultural Engineering,pp. 191-212.